PHYSICAL REVIEW C **76**, 042201(R) (2007)

# Measurement of the $\vec{\gamma} p \to K^+\Lambda$ reaction at backward angles

K. Hicks,[1] T. Mibe,[1] M. Sumihama,[2] D. S. Ahn,[2,3] J. K. Ahn,[3] H. Akimune,[4] Y. Asano,[5] W. C. Chang,[6] S. Daté,[7] H. Ejiri,[2,7] S. Fukui,[8] H. Fujimura,[9,10] M. Fujiwara,[2,11] S. Hasegawa,[2] A. Hosaka,[2] T. Hotta,[2] K. Imai,[9] T. Ishikawa,[12,9] T. Iwata,[13] B. Juliá-Díaz,[14] Y. Kato,[2] H. Kawai,[15] Z. Y. Kim,[10] K. Kino,[2,*] H. Kohri,[2] N. Kumagai,[7] T.-S. H. Lee,[16] S. Makino,[17] T. Matsuda,[18] T. Matsumura,[19] N. Matsuoka,[2] M. Miyabe,[9] Y. Miyachi,[8,†] M. Morita,[2] N. Muramatsu,[2] T. Nakano,[2] M. Niiyama,[9] M. Nomachi,[20] Y. Ohashi,[7] T. Ooba,[15] H. Ohkuma,[7] D. S. Oshuev,[6] S. Ozaki,[2] C. Rangacharyulu,[21] A. Sakaguchi,[20] T. Sasaki,[9] P. M. Shagin,[2,‡] Y. Shiino,[15] A. Shimizu,[2] H. Shimizu,[12] Y. Sugaya,[20,22] Y. Toi,[18] H. Toyokawa,[7] A. Wakai,[23,§] C. W. Wang,[6] S. C. Wang,[6,‖] K. Yonehara,[4,¶] T. Yorita,[7] M. Yoshimura,[24] M. Yosoi,[2,9] and R. G. T. Zegers[25]
(LEPS Collaboration)

[1]*Department of Physics and Astronomy, Ohio University, Athens, Ohio 45701, USA*
[2]*Research Center for Nuclear Physics, Osaka University, Ibaraki, Osaka 567-0047, Japan*
[3]*Department of Physics, Pusan National University, Busan 609-735, Korea*
[4]*Department of Physics, Konan University, Kobe, Hyogo 658-8501, Japan*
[5]*Synchrotron Radiation Research Center, Japan Atomic Energy Research Institute, Mikazuki, Hyogo 679-5198, Japan*
[6]*Institute of Physics, Academia Sinica, Taipei 11529, Taiwan*
[7]*Japan Synchrotron Radiation Research Institute, Mikazuki, Hyogo 679-5198, Japan*
[8]*Department of Physics and Astrophysics, Nagoya University, Nagoya, Aichi 464-8602, Japan*
[9]*Department of Physics, Kyoto University, Kyoto 606-8502, Japan*
[10]*School of Physics, Seoul National University, Seoul 151-747, Korea*
[11]*Kansai Photon Science Institute, Japan Atomic Energy Agency, Kizu, Kyoto 619-0215, Japan*
[12]*Laboratory of Nuclear Science, Tohoku University, Sendai, Miyagi 982-0826, Japan*
[13]*Department of Physics, Yamagata University, Yamagata 990-8560, Japan*
[14]*Departament de Estructura i Constituents de la Materia, Diagonal 647, 08028 Barcelona, Spain*
[15]*Department of Physics, Chiba University, Chiba 263-8522, Japan*
[16]*Physics Division, Argonne National Laboratory, Argonne, Illinois 60439, USA*
[17]*Wakayama Medical University, Wakayama 641-8509, Japan*
[18]*Department of Applied Physics, Miyazaki University, Miyazaki 889-2192, Japan*
[19]*Department of Applied Physics, National Defense Academy, Yokosuka 239-8686, Japan*
[20]*Department of Physics, Osaka University, Toyonaka, Osaka 560-0043, Japan*
[21]*Department of Physics and Engineering Physics, University of Saskatchewan, Saskatoon, Saskatchewan, Canada S7N 5E2*
[22]*Advanced Science Research Center, Japan Atomic Energy Research Institute, Tokai, Ibaraki 319-1195, Japan*
[23]*Center for Integrated Research in Science and Engineering, Nagoya University, Nagoya, Aichi 464-8603, Japan*
[24]*Institute for Protein Research, Osaka University, Suita, Osaka 565-0871, Japan*
[25]*National Superconducting Cyclotron Laboratory, Michigan State University, East Lansing, Michigan 48824-1321, USA*

(Received 30 July 2007; published 30 October 2007)

Cross sections for the $\gamma p \to K^+\Lambda$ reaction were measured at backward angles using linearly polarized photons in the range 1.50 to 2.37 GeV. In addition, the beam asymmetry for this reaction was measured for the first time at backward angles. The $\Lambda$ was detected at forward angles in the LEPS spectrometer via its decay to $p\pi^-$ and the $K^+$ was inferred using the technique of missing mass. These measurements, corresponding to kaons at far backward angles in the center-of-mass frame, complement similar CLAS data at other angles. Comparison with theoretical models shows that the reactions in these kinematics provide further opportunities to investigate the reaction mechanisms of hadron dynamics.

DOI: 10.1103/PhysRevC.76.042201 PACS number(s): 24.85.+p, 13.60.Le, 24.70.+s, 25.20.Lj

Measurements of the photoproduction of the $K^+\Lambda$ final state with high statistics have become possible in the past decade due to high-flux photon beams in the GeV range. Recently, the CLAS collaboration published a compendium of data for this reaction over a wide range of angles and photon energies [1]. One motivation for more complete $K^+\Lambda$ data is to study the details of $N^*$ resonances that were predicted

*Present address: Center for Nuclear Study, University of Tokyo, 7-3-1 Hongo, Bunkyo, Tokyo 113-0033, Japan.
†Present address: Department of Physics, Tokyo Institute of Technology, Tokyo 152-8551, Japan.
‡Present address: Department of Physics and Astronomy, Rice University, 6100 Main St., Houston MS 108, TX 77005-1892, USA.
§Present address: Akita Research Institute of Brain and Blood Vessels, Akita 010-0874, Japan.
‖Present address: Institute of Statistical Science, Academia Sinica, Nankang, 115 Taipei, Taiwan.
¶Present address: Illinois Institute of Technology, Chicago, IL 60616, USA.

 

to couple weakly to pion decay and more strongly to kaon decay. Some $N^*$ resonances that were predicted in quark models [2], but were not seen in partial wave analysis of pion scattering data, might be seen in kaon production. The CLAS data do not show definitive evidence for new $N^*$ resonances, but do exhibit a few broad energy-dependent structures in the differential cross sections, suggesting that there is a more complicated mechanism contributing to the $\gamma p \to K\Lambda$ reaction. The present results extend the existing data for $K^+\Lambda$ photoproduction to far backward kaon angles.

Theoretical progress for $K^+\Lambda$ photoproduction has been published recently [3] showing that coupled channel effects can no longer be ignored. This approach, the dynamical coupled-channels (DCC) formalism, includes a proper treatment of off-shell effects. The most important multistep transition, $\gamma N \to \pi N \to K\Lambda$, has a comparable cross section to direct production, $\gamma N \to K\Lambda$ [4]. In this case, the DCC formalism is necessary for a correct interpretation of $K^+\Lambda$ photoproduction data.

The CLAS detector acceptance does not allow measurements at either very forward or very backward kaon angles. Recently, the LEPS collaboration published cross sections for forward angles [5], showing good agreement with the CLAS data where the two data sets overlap. Here, cross sections for backward angles of this reaction are measured using a different experimental technique, where the $\Lambda$ is reconstructed from its decay products, which are detected in the LEPS spectrometer. The final state kaon, which goes backward in the center-of-mass frame, is measured through the missing mass technique.

In the kinematics that LEPS can access, we can study certain reaction dynamics selectively. For instance, in meson production at forward angles, $t$-channel diagrams dominate, and the nature of the exchange particle can be studied (see Ref. [6] for an example in $\phi$ photoproduction). In contrast, the far backward angles in meson photoproduction are associated with $u$-channel diagrams. In this article, we examine whether the data exhibit any $u$-channel signature in the cross sections.

At low energies, the $u$-channel amplitude is expected to be dominated by diagrams where a hyperon, such as a ground state $\Lambda$ or $\Sigma^0$, is exchanged. These diagrams are shown in Fig. 1. The coupling constants for the hadronic verticies in Fig. 1 are inferred from the $t$-channel in kaon photoproduction data, which are determined either by theoretical models (e.g., SU(3) symmetry) or by an independent fit in analyses

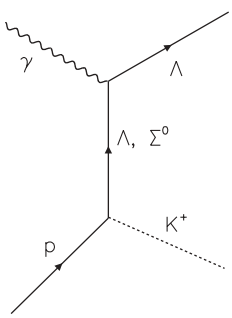


FIG. 1. Diagram of the $u$-channel for the reaction $\gamma p \to K^+\Lambda$ that contributes at backward kaon angles.

such as the DCC formalism for $\pi N \to KY$ reactions. The exchange baryon is neutral, and so the electromagnetic vertex is dominated by the $M1$ multipole, which acts to flip the spin of the $\Lambda$ or $\Sigma^0$. The magnetic moments of the $\Lambda$ and $\Sigma$ hyperons are known, so this vertex has little ambiguity. There is not much freedom in calculations of the diagram shown in Fig. 1.

Of course, we expect that there are further dynamical processes that may contribute to the reaction at this kinematical region. In the low energy regime, for instance, coupled-channel effects and nucleon resonances may be important as emphasized in Ref. [3]. The Regge model has also been used in the study of reactions in this energy region as well as with higher energy photons [7,8]. In this description, one can study the nature of baryon trajectories exchanged in the $u$ channel. The purpose of this article is to provide the cross sections and spin asymmetries at far backward angles and discuss reaction mechanisms that may be relevant to $u$-channel dynamics.

Direct detection of the $\Lambda$ provides additional information. At LEPS, the incident photon is highly polarized, and so the reaction plane of the $K^+\Lambda$ can be compared with the plane of the photon polarization, giving new information on the reaction mechanism. The beam asymmetry for kaon photoproduction has been measured at forward angles by LEPS [9] and is measured here in $u$-channel kinematics for the first time.

The experimental data were taken using the LEPS (laser electron photons at SPring-8) detector in Japan [10]. Ultraviolet light from an Ar laser was linearly polarized and directed onto the 8 GeV stored electron beam. Backward Compton scattering produced a narrow beam of photons up to 2.4 GeV. The struck electron was detected in a tagging spectrometer, giving the energy of individual photons in the range 1.5–2.4 GeV. The linear polarization of the photons is calculated for Compton scattering and was typically 97% at the maximum energy. The photon beam was incident on a 16-cm-long liquid hydrogen target. Details of the geometry are given elsewhere [5].

The LEPS spectrometer consists of a wide-gap dipole magnet, with charged-particle tracking detectors both before and after the magnet. An array of scintillator bars were placed 4 m downstream of the target and, along with a start counter (SC) scintillator 5 cm downstream of the target, provided a time-of-flight (TOF) measurement. The trigger was a coincidence between the tagger, the SC, and the TOF wall. Electron-positron pairs were vetoed by an aerogel cerenkov detector just after the SC.

The total number of photons on target was $1.18 \times 10^{12}$, after correcting for the transmission factor (for material between the beam production point and the target) and tagger inefficiencies.

Using momentum and TOF, the mass of each detected particle was measured, giving particle identification (PID). Events with a proton and a $\pi^-$, each having a measured mass within $3\sigma$ (where $\sigma$ is the momentum dependent mass resolution) of its known mass were kept for further analysis. The point of closest approach between these two tracks was calculated, and this vertex position was required to be within the target or downstream of the target. Because of the long lifetime of the $\Lambda$, the vertex position can be downstream of the target. A cut on vertex position before the SC was required in the analysis. Empty target runs showed that the contribution

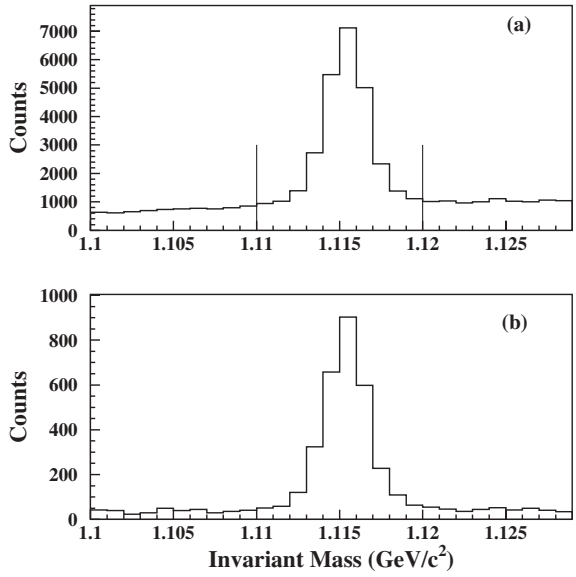


FIG. 2. Invariant mass of the $p\pi^-$ events, showing a peak for the $\Lambda$ riding on top of a smooth background: (a) raw data with a reconstructed vertex from the target, (b) with an additional requirement that the missing mass is a kaon.

of the target windows and the SC was less than about 4%. Monte Carlo simulations showed good agreement with the distribution of vertex position for events with $\Lambda \to p\pi^-$ decay in the experiment.

In addition to mass cuts, several additional requirements are used to ensure good PID. For example, when the track is extrapolated to the TOF wall, the position obtained from timing measurements on either end of the hit TOF bar must be within 8 cm of the expected position. The same PID requirements as described in Ref. [5] are used in the present analysis.

Figure 2 shows the invariant mass of the $p\pi^-$ pair (a) for all events with good PID and the above vertex cut and (b) for those events where the missing mass is consistent with the kaon mass. The smooth background in Fig. 2(a) likely comes from reactions like $\gamma p \to p\pi^+\pi^-$ where the $\pi^+$ is not detected. The spectrum in Fig. 2(b) has much less background because the missing particle is now required to have the mass of a $K^+$. The technique of sideband subtraction can be used to remove the remaining background. Let the $\Lambda$ region be given by a cut on the mass from 1.110 to 1.120 GeV/$c^2$ (shown by the vertical lines in Fig. 2). The left and right sideband regions on either side of the peak (of equal width) were analyzed in the same way as the $\Lambda$ region and subtracted from the final results.

The missing mass for the reaction $\gamma p \to \Lambda X$ is shown in Fig. 3 for six equal bins in the photon energy. The photon energy bins are 150 MeV wide, in six equal steps from 1.5 to 2.4 GeV. The number of photons in each energy bin was measured by the tagger, corrected for the inefficiencies of each tagger element. The plots in Fig. 3 are shown in order of increasing energy bin, from lowest (top left) to highest (lower right).

The data in Fig. 3 span the range $0.9 < \cos\theta_{\rm CM} < 1.0$, where $\theta_{\rm CM}$ is the center-of-mass (CM) polar angle of the $\Lambda$ momentum vector. These spectra have not yet been sideband subtracted, which mostly removes counts below a mass of 0.4 GeV/$c^2$. A clear peak is seen in the missing mass spectra at the value of the known $K^+$ mass. The strength at higher mass corresponds to a combination of $K\Sigma$ (followed by $\Sigma \to \Lambda\gamma$), $K^*\Lambda$, and $KY^*$ photoproduction.

The $K^+$ peak appears to decrease rapidly with increasing photon energy. These spectra are not corrected for the the acceptance for $\Lambda$ detection in the LEPS spectrometer, which is weakly dependent on photon energy. Data in a second angular bin, $0.8 < \cos\theta_{\rm CM} < 0.9$, are of similar quality and statistics.

The LEPS acceptance was calculated based on Monte Carlo simulations for $K^+\Lambda$ production uniformly distributed in energy and center-of-mass angle. More realistic distributions are possible, and studies with a phenomenological energy-dependent event generator showed that the systematic uncertainty of the acceptance is on the order of 4% or less. The simulations were carried out using the GEANT software [11] with input for the detector geometry and resolutions. A realistic Compton scattered photon beam distribution was used. The simulated peak widths for the invariant mass ($\Lambda$) and missing mass ($K^+$) are in good agreement with those shown in Figs. 2 and 3.

In addition to the $K^+\Lambda$ final state, the three reactions at higher missing mass mentioned above ($K\Sigma$, $K^*\Lambda$, $KY^*$) were simulated along with a general three-body phase space for the $K\pi\Lambda$ final state. Missing mass spectra from all of the simulations were used as input to a template fit of the experimental data, where each template spectrum was multiplied by an overall factor to minimize the reduced $\chi^2$, which was typically in the range of 1–2. The number of counts in the $K^+$ peak was extracted from the template fits. The $K^+$ fit is affected primarily by background from the $K^+\Sigma^0$ reaction, which was constrained largely by the events at masses about 0.1 GeV/$c^2$ higher than the $K^+$ peak. Simulations show that the other reactions, including three-body phase space, have significant strength only at higher missing mass than for $K\Sigma$.

The systematic uncertainty of the fitting procedure was estimated by doing fits with Gaussians for the background of $K\Sigma$ production and of the three-body final states at higher missing mass. Comparison of the Gaussian and template fit results gives a mean systematic uncertainty of 5%. Other systematic uncertaintes due to target thickness, photon flux, and event selection cuts added in quadrature contribute 4%. The overall systematic uncertainty, including that of the Monte Carlo simulations, is 7.5%.

For three photon energy ranges, see Fig. 4, the cross section was binned for several values of $u = (p_\gamma - p_\Lambda)^2$. The maximum value, $u_{\rm max}$ occurs when the $\Lambda$ goes forward at 0° from the photon direction. The cross sections in Fig. 4 are shown as a function of $u - u_{\rm max}$. Theoretical calculations [12] for the $u$ channel only, shown by the solid line, are far below the data and suggest that the diagram of Fig. 1 is not dominant. These calculations include exchange baryons of $\Lambda$, $\Sigma^0$, and $\Sigma(1385)$ along with a form factor with a cutoff mass of about 0.9 GeV (the theoretical values increase for higher cutoff mass). It appears that $s$-channel diagrams still contribute strongly to the cross section even at these far backward kaon angles, at least at the lower photon energies.

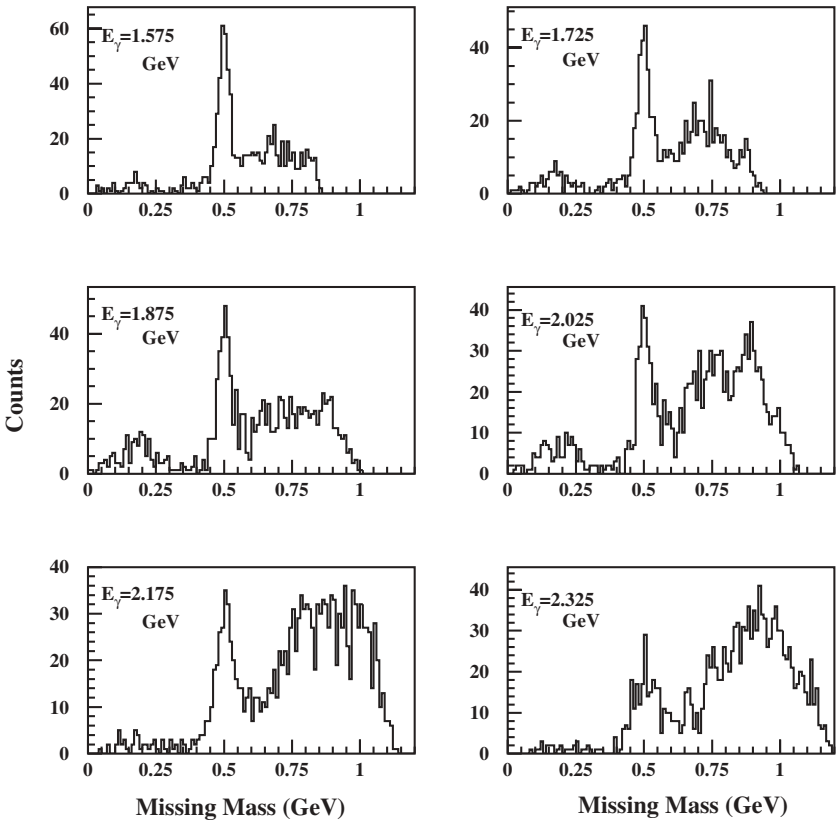


FIG. 3. Missing mass of the $\gamma p \to \Lambda X$ reaction for the angular bin $0.90 < \cos\theta_{\rm CM} < 1.0$, where $\theta_{\rm CM}$ is the center-of-mass angle of the $\Lambda$. Each figure is for the photon energy shown by the label.

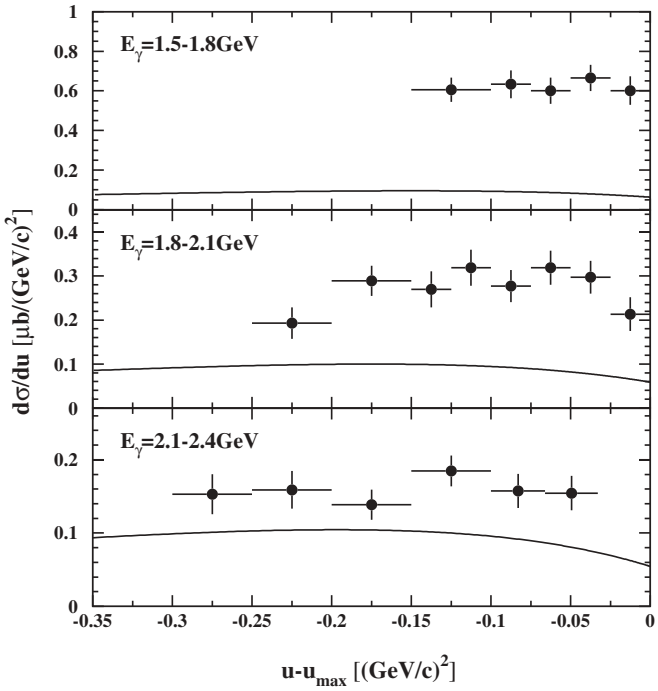


FIG. 4. Differential cross sections as a function of the Mandelstam variable $u$ for the given photon beam energy. The curves are calculations of the contribution from the diagram in Fig. 1 only, using exchange of $\Lambda$, $\Sigma^0$, and $\Sigma^*$ hyperons.

At photon energies above 4.3 GeV, $K^+\Lambda$ data clearly show a rise for $u$ between $-0.2$ and $-0.7$ $(\mathrm{GeV/c})^2$ [13], but the present data do not exhibit this $u$-channel signature. The fact that the cross sections are nearly constant as a function of $u - u_{\rm max}$ can be interpreted as additional evidence for the lack of dominance by the $u$-channel diagram of Fig. 1 for backward angle $K^+\Lambda$ data at photon energies below about 3 GeV.

Differential cross sections as a function of six photon energy bins, for each of two $\Lambda$ angle bins (see above), are plotted in Fig. 5. Here, the cross sections are presented in the same format as that used for the CLAS data [1]. The angle-dependent acceptance ranged from about 2 to 3% in the lowest energy bin up to 6–8% at the highest energy bin.

Because the $u$-channel diagram alone cannot explain the present data, theoretical curves from Ref. [3] are shown in Fig. 5, converted to the present units. The hatched region is for the full DCC model, showing the variation of this calculation over the angular range of the bin, whereas the dashed curves do not include DCC effects (see Fig. 14 of Ref. [3]). The present data are closer to the full DCC calculation, except for one point at the lowest photon energy ($E_\gamma = 1.575$ GeV) and most backward kaon angle. The top plot, for $\cos\theta_{\rm CM} = 0.85$ agrees within error bars with the CLAS data, which is conveniently tabulated in Ref. [1] but not shown in Fig. 5. The lower plot, for $\cos\theta_{\rm CM} = 0.95$, goes beyond the angular region covered by CLAS. In general the data follow the energy and angle dependence predicted by the DCC model, but are still significantly different in the range of $E\gamma = 2.0$–2.2 GeV.

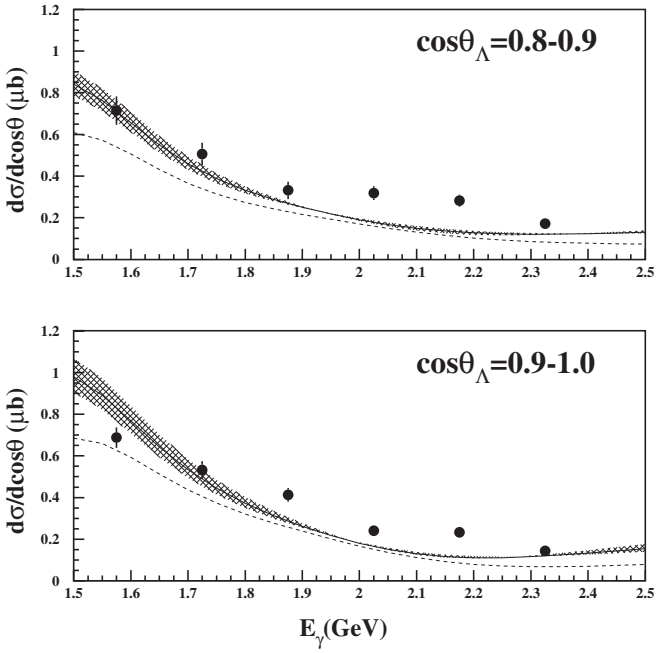


FIG. 5. Differential cross sections at the angle shown as a function of photon beam energy. Calculations in the model of Ref. [3] are shown without (dashed) and with (hatched region) coupled channels.

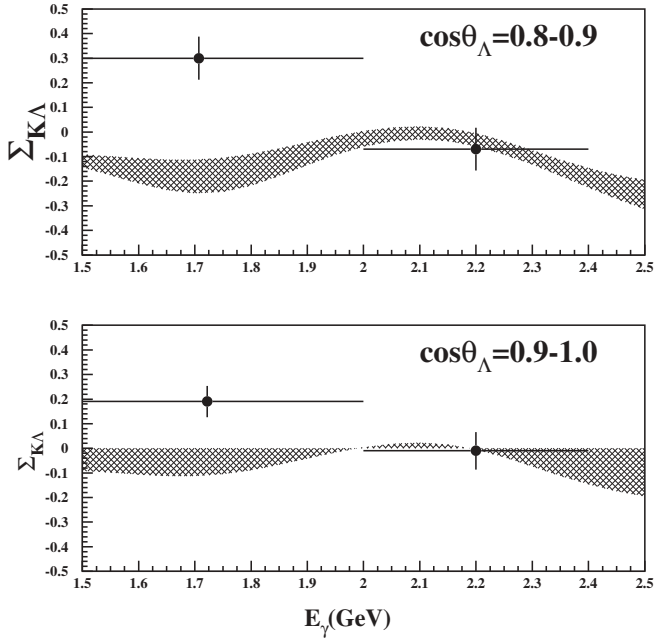


FIG. 6. Beam asymmetry at the angles shown as a function of photon beam energy. The points have been averaged over the range of photon energy shown. Calculations in the model of Ref. [3] with coupled channels (hatched region) are shown for comparison.

Alternatively, we performed a simple estimation using the Regge model, where we fit the energy dependence by an exponential function,

$$\frac{d\sigma}{du} \propto s^{-2(\alpha(0)-1)},$$

where $\alpha(0)$ is the intercept for the hyperon trajectory exchanged in the $u$ channel. By choosing $\alpha(0) = -0.84$, the energy dependence can be fit and extrapolated to the previous data at 4.3 GeV [13]. This value of $\alpha(0)$ is not too far from the value $-0.68$ extrapolated from the mass dependence of the $\Lambda^*$ resonances [7].

Figure 6 shows the beam asymmetry, which was measured by binning the $K^+\Lambda$ data as a function of $\phi$, which is defined as the azimuthal angle of the $\Lambda$ as measured from the linear polarization plane of the photon beam. To gain sufficient statistics for the $\phi$ fit, only two bins in photon energy were used, one from 1.5 to 2.0 GeV and a second one from 2.0 to 2.4 GeV. The data are plotted at the cross-section weighted energy (rather than the bin center). We follow the same procedure to extract the beam asymmetry as described previously [9]. The data were averaged over the entire bin size for the fits shown and were also averaged over smaller bin sizes to ensure that the results for the full bin were consistent with a weighted average. In particular, the asymmetry goes to zero at $\cos\theta^* = 1.0$ and indeed the data follow this trend. A positive beam asymmetry, $\Sigma_{K\Lambda}$, is seen in the first energy bin, and a slightly negative asymmetry is seen at higher photon energy. The positive asymmetry means that more $K^+\Lambda$ reactions are produced perpendicular to the linear polarization direction (i.e., parallel to the magnetic field of the photon) than parallel to the beam polarization. Physically, when the magnetic interaction dominates, the asymmetry becomes positive, while if the electric interaction dominates, it becomes negative.

The DCC model, shown by the hatched region (with the same meaning as in Fig. 5), predicts a slightly negative polarization over most of the photon energy range in Fig. 6. These results will constrain the backward angle predictions of theoretical models, which were largely unconstrained until now. In contrast to Ref. [9], where the beam asymmetry increases with increasing photon energy, here we see that $\Sigma_{K\Lambda}$ decreases with photon energy. As shown in Fig. 11 of Ref. [3], where calculations are done without the inclusion of various $N^*$ resonances, the backward angle beam asymmetry is strongly affected by the inclusion of a third $D_{13}$ resonance (at 1954 MeV). The data in Fig. 6 at lower photon energies agree better with calculations that do not include this third $D_{13}$ resonance. However, conclusive results can only be obtained by including the new data in overall fits to all $K\Lambda$ photoproduction data.

In summary, measurements of forward angle $\Lambda$ production were carried out at the LEPS spectrometer at SPring-8. These data correspond to backward angle kaons in the CM frame. The data are in good agreement with CLAS data [1], where the angular ranges overlap, and go beyond the CLAS angles to far backward angles.

The cross sections agree with the general trend of the calculations in the DCC model [3] but are significantly higher around $E_\gamma = 2.1$ GeV. The Regge model can explain the energy dependence of the present data and even be extrapolated to previous data at 4.3 GeV, whereas the effective Lagrangian models cannot reproduce the data over this range of photon energies. The beam asymmetries show a positive sign at photon

energies below 2.0 GeV, in contrast with theoretical predictions of the DCC model.

Meson photoproduction at backward angles (and to some extent forward angles as well) has not been explored much so far. Therefore, the present data are useful to constrain various models of strangeness production. In the present article, we have shown that coupled-channels effects are important and that some resonance nature, with mass around 2 GeV, may be studied in the DCC model [3]. In particular, the $D_{13}$ in the $s$ channel was shown to affect the cross sections. The Regge model can also provide information of hyperon trajectories, which have not been fully studied for the $u$ channel. Further experiments on kaon photoproduction and other mesons at backward angles will stimulate further theoretical progress.

The authors thank the SPring-8 staff for supporting the BL33LEP beam line and the LEPS experiment. We thank H. Toki (RCNP) for fruitful discussions. This research was supported in part by the Ministry of Education, Science, Sports and Culture of Japan, by the National Science Council of Republic of China (Taiwan), Korea Research Foundation (KRF) Grant 2006-312-C00507, MEC (Spain) Grant FIS2005-03142, the European Hadron Physics Project (RII3-CT-2004-506078), and the National Science Foundation (NSF Award PHY-0555558).

[1] R. Bradford *et al.* (CLAS Collaboration), Phys. Rev. C **73**, 035202 (2006).
[2] S. Capstick and W. Roberts, Phys. Rev. D **58**, 074011 (1998).
[3] B. Juliá-Díaz, B. Saghai, T.-S. H. Lee, and F. Tabakin, Phys. Rev. C **73**, 055204 (2006).
[4] W.-T. Chiang, F. Tabakin, T.-S. H. Lee, and B. Saghai, Phys. Lett. **B517**, 101 (2001).
[5] M. Sumihama *et al.* (LEPS Collaboration), Phys. Rev. C **73**, 035214 (2006).
[6] T. Mibe *et al.* (LEPS Collaboration), Phys. Rev. Lett. **95**, 182001 (2005).
[7] M. Guidal, Ph.D. thesis, University of Orsay, 1997.
[8] T. Mart, S. Sulaksono, and C. Bennhold, in *Proceedings of the International Symposium on the Electroproduction of Strangeness on Nucleons and Nuclei,* edited by K. Maeda (World Scientific, Singapore, 2004).
[9] R. G. T. Zegers *et al.* (LEPS Collaboration), Phys. Rev. Lett. **91**, 092001 (2003).
[10] T. Nakano *et al.*, Nucl. Phys. **A684**, 71 (2001).
[11] R. Brun, Applications Software Group, Long Writeup W5013, CERN, Geneva, Switzerland.
[12] S. Ozaki and A. Hosaka (private communication).
[13] R. L. Anderson *et al.*, Phys. Rev. Lett. **23**, 890 (1969).